Transceiver Design for MIMO AF Relay Systems with a PS Based Wireless Powered Relay Node

Yue Rong
School of Electrical Engineering, Computing and Mathematical Sciences, Curtin University, Bentley, WA, Australia
E-mail: y.rong@curtin.edu.au

***Abstract*—In this article, we consider a dual-hop multiple-input multiple-output (MIMO) amplify-and-forward (AF) relay system, where the relay node harvests the radio frequency energy from the signals transmitted from the source node, and then utilizes the harvested energy to forward source signals to the destination node. In particular, the power splitting (PS) protocol is adopted by the relay node for energy harvesting and information receiving. We employ a general sum power constraint at the relay node and investigate the joint design of the source matrix, the relay matrix, and the PS ratios to maximize the system mutual information (MI). We establish the structure of the source matrix and the relay matrix, which simplifies the complicated transceiver design problem with matrix variables to a power distribution problem with scalar variables. We propose two approaches to efficiently solve the resulting power allocation problem with performance-complexity tradeoffs. Numerical simulations demonstrate that the proposed methods yield a higher system MI than existing approaches.**

***Index Terms*—Energy harvesting, power splitting receiver, multiple-input multiple-output relay, amplify-and-forward relay.**

I. Introduction

A key factor which limits the performance of wireless devices is the life time and energy constraints. To overcome this challenge, a new technology applying radio frequency (RF) signals to transfer energy to wireless devices has been developed [1]. To coordinate the wireless information transmission (WIT) and wireless energy transfer (WET), time switching (TS) and power splitting (PS) protocols have been developed in [2].

Multiple-input multiple-output (MIMO) and relay communication techniques can increase the system energy efficiency and spectral efficiency [3], [4]. By installing multiple transmit antennas at nodes of a wireless network, RF energy can be more effectively delivered to wireless nodes compared with nodes having only a single antenna, and thus, the life time of energy limited wireless systems is effectively extended [2].

The application of wireless powered communication (WPC) in MIMO relay systems has been studied in [5]-[13]. In [5], an amplify-and-forward (AF) space-time block code (OSTBC) based MIMO relay system with a multi-antenna energy harvesting (EH) receiver has been investigated. Under several receiver architectures, energy-rate trade-offs by applying the EH technique in MIMO relay communication systems have been studied in [6]. PS and TS protocols have been proposed in [7] for a MIMO AF relay communication system, where the joint source matrix and relay matrix optimization has been considered to optimize the system rate. Transceiver optimization for AF MIMO relay systems employing an energy harvesting relay node has been studied in [11]. In [12], DF MIMO relay systems with a wireless powered relay node have been investigated. A hybridized power time spitting based relaying protocol has been proposed in [13] for MIMO relay systems.

In this work, we study a dual-hop MIMO AF relay communication system, where a receiver with EH capability is applied at the relay to facilitate the energy and information transmission. Relay nodes are particularly useful in systems where the direct source-destination channel is much weaker than the channel through the relay node due to shadowing and path attenuation by obstacles [5], [7], [11]. We apply the PS protocol in this paper, where signals received at the relay node are split into two portions. One part of the signals are linearly precoded and forwarded to the destination node by utilizing the energy harvested from the other part of the signals.

It is assumed in [7] that the energy harvested on one subchannel of the source-relay link is only utilized for the information forwarding on one subchannel. Here, we depart from this strict per data stream power constraint and propose a more general sum power constraint at the relay node. Compared with the formulation in [7], the total harvested energy at the relay node over all subchannels can be used to forward signals at all subchannels. Thus, the sum energy constraint in this paper is more general and includes the per data stream energy constraints adopted in [7] as special cases. Therefore, we can expect a better system performance.

We study the joint design of the source matrix, relay matrix, and the PS ratios to maximize the system mutual information (MI), under the power constraint at the source node and the proposed sum harvested energy constraint at the relay node. Note that the transceiver design problem in this paper is much more challenging to solve compared with the problem in [7]. We derive the structure of the source matrix and the relay matrix, which reduces the complex-valued matrix optimization variables to scalar power allocation optimization variables. We develop two approaches to solve the resulting power allocation problem. In particular, the first algorithm solves the original nonconvex power allocation problem using the sequential quadratic programming (SQP) method [14], while the other algorithm converts the original problem to a convex problem by using a tight upper bound of the system MI function. In particular, we demonstrate that the optimal power allocation problem based on the upper bound can be converted to a nonlinear semidefinite programming (SDP) problem, which is solvable through the disciplined convex programming toolbox CVX [15]. We demonstrate through numerical simulations that the two proposed algorithms have a higher system rate than that in [7]. Moreover, the first method has a slightly higher MI than the second method, at the cost of a higher computational complexity.

The remainder of this article is organized as below. The system model of a MIMO AF relay system employing a wireless powered relay node is introduced in Section II. The joint transceiver design problem is also formulated in this section. In Section III, two algorithms are presented to solve the source and relay design problem. Numerical simulations are carried out in Section IV to compare the performance of existing approaches with our proposed transceiver design algorithms. Finally, we draw conclusions in Section V.

II. System Model

We investigate a dual-hop three-node MIMO communication network where a source node communicates with a destination node via a relay node as illustrated in Fig. 1. The number of antennas equipped at the source, relay, and destination nodes are N_s, N_r, and N_d, respectively. It is assumed that the source node and the destination node have constant power supply, however the relay node obtains its power from harvesting the RF energy carried by the signals sent from the source node. One source-destination communication cycle is completed in two phases with equal duration. During the first phase, information and energy carrying signals are sent by the source node to the relay node, and the relay node adopts the PS protocol [2] to harvest energy from the received source signals.

For the second phase, the information-bearing signals received by the relay node are multiplied by a precoding matrix and forwarded to the destination node [7]. Among different relay protocols at the relay node, we choose the AF scheme thanks to its shorter processing delay and implementation simplicity. Moreover, in contrast to regenerative relay protocols, in the AF relay protocol, the relay node does not need to decode and then re-encode information signals. Thus, the amount of signal processing and coding work at the relay node is smaller in an AF relay system. This reduces the power consumption of the relay node and makes the AF scheme suitable for wireless-powered relay nodes. Following [5], [7], and [11], the direct source-destination channel is neglected, as compared with the link through the relay node, the effect of path shadowing and attenuation is more severe on the direct channel.

During the first phase, an $N_1 \times 1$ source signal $\mathbf{s}$ is multiplied by an $N_s \times N_1$ source matrix $\mathbf{B}$. Then the precoded vector is sent to the relay node. It is assumed that $E\{\mathbf{s}\mathbf{s}^H\} = \mathbf{I}_{N_1}$, where $E\{\cdot\}$ is the statistical expectation, $\mathbf{I}_n$ is an $n \times n$ identity matrix, and $(\cdot)^H$ represents the Hermitian transpose. The signal received by the relay node can be written as

$$\mathbf{y}_r = \mathbf{H}\mathbf{B}\mathbf{s} + \mathbf{v}_r \tag{1}$$

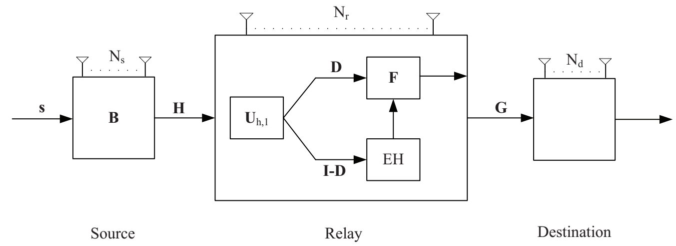

Fig. 1. A dual-hop MIMO AF relay system with a PS based wireless powered relay node.

where $\mathbf{H}$ is an $N_r \times N_s$ source-relay MIMO channel, and $\mathbf{v}_r$ is an additive white Gaussian noise (AWGN) at the relay node with zero-mean and $E\{\mathbf{v}_r\mathbf{v}_r^H\} = \sigma_r^2\mathbf{I}_{N_r}$.

The relay node first multiplies $\mathbf{y}_r$ by $\mathbf{U}_{h,1}^H$ [7, p. 1601], where $\mathbf{H} = \mathbf{U}_h\mathbf{\Lambda}_h^{\frac{1}{2}}\mathbf{V}_h^H$ represents the singular value decomposition (SVD) of the channel $\mathbf{H}$ with the diagonal elements of $\mathbf{\Lambda}_h$ arranged in a decreasing order, and $\mathbf{U}_{h,1}$ contains the leftmost N_1 columns of $\mathbf{U}_h$. From (1), we have

$$\mathbf{z}_r = \mathbf{U}_{h,1}^H\mathbf{y}_r = \mathbf{\Lambda}_{h,1}^{\frac{1}{2}}\mathbf{V}_{h,1}^H\mathbf{B}\mathbf{s} + \mathbf{U}_{h,1}^H\mathbf{v}_r \tag{2}$$

where $\mathbf{\Lambda}_{h,1}$ contains the largest N_1 singular values of $\mathbf{H}$ and $\mathbf{V}_{h,1}$ contains the leftmost N_1 columns of $\mathbf{V}_h$.

By applying the PS protocol, the relay node first splits the signal $\bar{\mathbf{z}}_r \triangleq \mathbf{\Lambda}_{h,1}^{\frac{1}{2}}\mathbf{V}_{h,1}^H\mathbf{B}\mathbf{s}$ with an $N_1 \times N_1$ PS matrix $\mathbf{D} = \text{diag}(d_1, \cdots, d_{N_1})$, where $\mathbf{D}^{\frac{1}{2}}\bar{\mathbf{z}}_r$ is for information transmission and $(\mathbf{I}_{N_1} - \mathbf{D})^{\frac{1}{2}}\bar{\mathbf{z}}_r$ is used for the energy harvesting. Note $\text{diag}(\cdot)$ represents a diagonal matrix and $0 \leq d_i \leq 1$, $i = 1, \cdots, N_1$, denotes the PS ratio for the ith data stream. Following [7], the RF energy harvested at the relay node can be written as

$$\begin{aligned} E_r &= \eta E\{\text{tr}((\mathbf{I}_{N_1} - \mathbf{D})^{\frac{1}{2}}\bar{\mathbf{z}}_r\bar{\mathbf{z}}_r^H(\mathbf{I}_{N_1} - \mathbf{D})^{\frac{1}{2}})\} \\ &= \eta\text{tr}((\mathbf{I}_{N_1} - \mathbf{D})\tilde{\mathbf{B}}\tilde{\mathbf{B}}^H) \end{aligned} \tag{3}$$

where $\tilde{\mathbf{B}} \triangleq \mathbf{\Lambda}_{h,1}^{\frac{1}{2}}\mathbf{V}_{h,1}^H\mathbf{B}$, $\text{tr}(\cdot)$ is the matrix trace and $0 < \eta < 1$ is the efficiency of energy conversion.

The signal vector transmitted by the relay node is given by

$$\mathbf{x}_r = \mathbf{F}\mathbf{D}^{\frac{1}{2}}\tilde{\mathbf{B}}\mathbf{s} + \mathbf{F}\mathbf{U}_{h,1}^H\mathbf{v}_r \tag{4}$$

where $\mathbf{F}$ is a $N_r \times N_1$ relay precoding matrix. Based on (4), the signal vector received at the destination node is given by

$$\begin{aligned} \mathbf{y}_d &= \mathbf{G}\mathbf{x}_r + \mathbf{v}_d \\ &= \mathbf{G}\mathbf{F}\mathbf{D}^{\frac{1}{2}}\tilde{\mathbf{B}}\mathbf{s} + \mathbf{G}\mathbf{F}\mathbf{U}_{h,1}^H\mathbf{v}_r + \mathbf{v}_d \end{aligned} \tag{5}$$

where $\mathbf{G}$ is an $N_d \times N_r$ relay-destination MIMO channel matrix, and $\mathbf{v}_d$ is the AWGN vector at the destination node with zero-mean and $E\{\mathbf{v}_d\mathbf{v}_d^H\} = \sigma_d^2\mathbf{I}_{N_d}$. From (5), the MI between the source and destination nodes can be written as

$$\begin{aligned} \text{MI}(\mathbf{D}, \mathbf{B}, \mathbf{F}) = \frac{1}{2}\log|&\mathbf{I}_{N_1} + \tilde{\mathbf{B}}^H\mathbf{D}^{\frac{1}{2}}\mathbf{F}^H\mathbf{G}^H \\ &\times(\sigma_r^2\mathbf{G}\mathbf{F}\mathbf{F}^H\mathbf{G}^H + \sigma_d^2\mathbf{I}_{N_d})^{-1}\mathbf{G}\mathbf{F}\mathbf{D}^{\frac{1}{2}}\tilde{\mathbf{B}}| \end{aligned} \tag{6}$$

where $(\cdot)^{-1}$ and $|\cdot|$ stand for the matrix inversion and matrix determinant, respectively.

It is assumed that $\mathbf{H}$ and $\mathbf{G}$ are quasi-static block fading, and the channel state information (CSI) of $\mathbf{H}$ and $\mathbf{G}$ is known. We also assume that $\mathrm{rank}(\mathbf{F}) = \mathrm{rank}(\mathbf{B}) = N_1$ and $N_1 \leq \min(\mathrm{rank}(\mathbf{H}), \mathrm{rank}(\mathbf{G}))$, where $\mathrm{rank}(\cdot)$ is the matrix rank. From (4), the energy consumption at the relay to forward $\mathbf{x}_r$ to the destination is represented as

$$\mathrm{tr}(E\{\mathbf{x}_r\mathbf{x}_r^H\}) = \mathrm{tr}(\mathbf{F}(\mathbf{D}^{\frac{1}{2}}\tilde{\mathbf{B}}\tilde{\mathbf{B}}^H\mathbf{D}^{\frac{1}{2}} + \sigma_r^2\mathbf{I}_{N_r})\mathbf{F}^H). \quad (7)$$

According to (3) and (7), the energy constraint at the relay is given by

$$\mathrm{tr}(\mathbf{F}(\mathbf{D}^{\frac{1}{2}}\tilde{\mathbf{B}}\tilde{\mathbf{B}}^H\mathbf{D}^{\frac{1}{2}} + \sigma_r^2\mathbf{I}_{N_r})\mathbf{F}^H) \leq \eta\mathrm{tr}((\mathbf{I}_{N_1} - \mathbf{D})\tilde{\mathbf{B}}\tilde{\mathbf{B}}^H). \quad (8)$$

From (6) and (8), the transceiver design problem for the proposed MIMO AF relay system with a PS based EH relay node can be written as

$$\max_{\mathbf{D},\mathbf{B},\mathbf{F}} \ \mathrm{MI}(\mathbf{D},\mathbf{B},\mathbf{F}) \quad (9a)$$

$$\text{s.t.} \ \mathrm{tr}(\mathbf{B}\mathbf{B}^H) \leq P \quad (9b)$$

$$\mathrm{tr}(\mathbf{F}(\mathbf{D}^{\frac{1}{2}}\tilde{\mathbf{B}}\tilde{\mathbf{B}}^H\mathbf{D}^{\frac{1}{2}} + \sigma_r^2\mathbf{I}_{N_r})\mathbf{F}^H) \leq \eta\mathrm{tr}((\mathbf{I}_{N_1} - \mathbf{D})\tilde{\mathbf{B}}\tilde{\mathbf{B}}^H) \quad (9c)$$

$$0 \leq d_i \leq 1, \quad i = 1, \cdots, N_1 \quad (9d)$$

where P is the power available at the source. Note that (9c) is the sum power constraint across all data streams, while in [7], a power constraint is imposed on each data stream. Thus, the problem (9) has a larger feasible region than the problem in [7]. Hence, transceivers designed under the problem (9) are expected to have a higher system MI than those in [7]. This will be shown further in next sections.

III. Proposed Algorithms

The system design problem (9) is nonconvex with matrix variables. In particular, the complicated objective function in (9a) and the constraint in (9c) make problem (9) difficult to solve. In this section, we first establish the structure of $\mathbf{B}$ and $\mathbf{F}$. Using this structure, the problem (9) can be converted to a simpler power allocation problem. Then we propose two methods to solve this problem. Let us introduce

$$\mathbf{G} = \mathbf{U}_g\mathbf{\Lambda}_g^{\frac{1}{2}}\mathbf{V}_g^H \quad (10)$$

as the SVD of $\mathbf{G}$, where the diagonal elements of $\mathbf{\Lambda}_g$ are arranged in a decreasing order.

Theorem 1: As the solution to the transceiver design problem (9), the optimal source matrix $\mathbf{B}$ and relay matrix $\mathbf{F}$ have the following structure

$$\mathbf{B}^* = \mathbf{V}_{h,1}\mathbf{\Lambda}_b^{\frac{1}{2}}\mathbf{U}^H, \quad \mathbf{F}^* = \mathbf{V}_{g,1}\mathbf{\Lambda}_f^{\frac{1}{2}} \quad (11)$$

where $(\cdot)^*$ represents the optimal value, $\mathbf{\Lambda}_b$ and $\mathbf{\Lambda}_f$ are $N_1 \times N_1$ diagonal matrices, $\mathbf{U}$ is an $N_1 \times N_1$ unitary matrix, and $\mathbf{V}_{g,1}$ contain the leftmost N_1 columns of $\mathbf{V}_g$.

Proof: See Appendix. □

It can be observed from (11) that the optimal $\mathbf{B}$ and $\mathbf{F}$ have a similar structure to the source and relay matrices in a two-hop MIMO AF relay system with a self-powered relay node [19]. Substituting (11) into (9), the transceiver optimization problem (9) can be rewritten as

$$\max_{\mathbf{\Lambda}_b,\mathbf{\Lambda}_f,\mathbf{D}} \ \log|\mathbf{I}_{N_1} + \mathbf{\Lambda}_{g,1}\mathbf{\Lambda}_f\mathbf{D}\mathbf{\Lambda}_{h,1}\mathbf{\Lambda}_b \times(\sigma_r^2\mathbf{\Lambda}_{g,1}\mathbf{\Lambda}_f + \sigma_d^2\mathbf{I}_{N_1})^{-1}| \quad (12a)$$

$$\text{s.t.} \ \mathrm{tr}(\mathbf{\Lambda}_b) \leq P \quad (12b)$$

$$\mathrm{tr}(\mathbf{\Lambda}_f(\mathbf{D}\mathbf{\Lambda}_{h,1}\mathbf{\Lambda}_b + \sigma_r^2\mathbf{I}_{N_1})) \leq \eta\mathrm{tr}((\mathbf{I}_{N_1} - \mathbf{D})\mathbf{\Lambda}_{h,1}\mathbf{\Lambda}_b) \quad (12c)$$

$$0 \leq d_i \leq 1, \quad i = 1, \cdots, N_1 \quad (12d)$$

where $\mathbf{\Lambda}_{g,1}$ contains the largest N_1 singular values of $\mathbf{G}$. As $\mathbf{\Lambda}_{g,1}$, $\mathbf{\Lambda}_f$, $\mathbf{D}$, $\mathbf{\Lambda}_{h,1}$, and $\mathbf{\Lambda}_b$ are diagonal matrices, the problem (12) is equivalent to the following problem

$$\max_{\mathbf{d},\boldsymbol{\lambda}_b,\boldsymbol{\lambda}_f} \ \sum_{i=1}^{N_1}\log\left(1 + \frac{d_i\lambda_{b,i}\lambda_{h,i}\lambda_{f,i}\lambda_{g,i}}{1 + \lambda_{f,i}\lambda_{g,i}}\right) \quad (13a)$$

$$\text{s.t.} \ \sum_{i=1}^{N_1}\lambda_{b,i} \leq P \quad (13b)$$

$$\sum_{i=1}^{N_1}\lambda_{f,i}(d_i\lambda_{h,i}\lambda_{b,i} + 1) \leq \eta\sum_{i=1}^{N_1}(1 - d_i)\tilde{\lambda}_{h,i}\lambda_{b,i} \quad (13c)$$

$$0 \leq d_i \leq 1, \ \lambda_{b,i} \geq 0, \ \lambda_{f,i} \geq 0, \ i = 1, \cdots, N_1 \quad (13d)$$

where $\mathbf{d} = [d_1, \cdots, d_{N_1}]^T$, $\boldsymbol{\lambda}_b = [\lambda_{b,1}, \cdots, \lambda_{b,N_1}]^T$, $\boldsymbol{\lambda}_f = [\lambda_{f,1}, \cdots, \lambda_{f,N_1}]^T$, $\lambda_{h,i} = \tilde{\lambda}_{h,i}/\sigma_r^2$, $\lambda_{g,i} = \tilde{\lambda}_{g,i}/\sigma_d^2$, $\lambda_{f,i} = \tilde{\lambda}_{f,i}\sigma_r^2$, $\lambda_{b,i}$, $\tilde{\lambda}_{f,i}$, $\tilde{\lambda}_{h,i}$, $\tilde{\lambda}_{g,i}$ are the ith diagonal element of $\mathbf{\Lambda}_b$, $\mathbf{\Lambda}_f$, $\mathbf{\Lambda}_h$ and $\mathbf{\Lambda}_g$, respectively, and $(\cdot)^T$ denotes the matrix transpose.

By introducing $a_i = \lambda_{h,i}$, $b_i = \lambda_{g,i}$, $x_i = \lambda_{b,i}$, $y_i = \lambda_{f,i}(d_i\lambda_{h,i}\lambda_{b,i} + 1)$, $i = 1, \cdots, N_1$, the power allocation problem (13) can be rewritten as

$$\max_{\mathbf{d},\mathbf{x},\mathbf{y}} \ \sum_{i=1}^{N_1}\log\left(1 + \frac{d_ia_ix_ib_iy_i}{1 + d_ia_ix_i + b_iy_i}\right) \quad (14a)$$

$$\text{s.t.} \ \sum_{i=1}^{N_1}x_i \leq P \quad (14b)$$

$$\sum_{i=1}^{N_1}y_i \leq \eta\sum_{i=1}^{N_1}\sigma_r^2(1 - d_i)a_ix_i \quad (14c)$$

$$0 \leq d_i \leq 1, \ x_i \geq 0, \ y_i \geq 0, \quad i = 1, \cdots, N_1 \quad (14d)$$

where $\mathbf{x} = [x_1, \cdots, x_{N_1}]^T$ and $\mathbf{y} = [y_1, \cdots, y_{N_1}]^T$. Let us introduce $w_i = d_ix_i$, $i = 1, \cdots, N_1$, the problem (14) can be equivalently converted to

$$\max_{\mathbf{w},\mathbf{x},\mathbf{y}} \ \sum_{i=1}^{N_1}\log\left(1 + \frac{a_iw_ib_iy_i}{1 + a_iw_i + b_iy_i}\right) \quad (15a)$$

$$\text{s.t.} \ \sum_{i=1}^{N_1}x_i \leq P \quad (15b)$$

$$\sum_{i=1}^{N_1}y_i \leq \eta\sum_{i=1}^{N_1}\sigma_r^2a_i(x_i - w_i) \quad (15c)$$

$$x_i \geq w_i \geq 0, \ y_i \geq 0, \quad i = 1, \cdots, N_1 \quad (15d)$$

where $\mathbf{w} = [w_1, \cdots, w_{N_1}]^T$. In the sequel, we propose two methods to solve the problem (15), which provide performance-complexity tradeoffs.

A. Proposed Method 1

By introducing $\frac{a_i w_i b_i y_i}{1+a_i w_i + b_i y_i} \geq t_i,\ i = 1, \cdots, N_1$, the problem (15) can be equivalently rewritten as

$$\max_{\mathbf{w},\mathbf{x},\mathbf{y},\mathbf{t}} \sum_{i=1}^{N_1} \log(1+t_i) \tag{16a}$$

$$\text{s.t. } \frac{a_i w_i b_i y_i}{1+a_i w_i + b_i y_i} \geq t_i,\ i = 1, \cdots, N_1 \tag{16b}$$

$$\sum_{i=1}^{N_1} x_i \leq P \tag{16c}$$

$$\sum_{i=1}^{N_1} y_i \leq \eta \sum_{i=1}^{N_1} \sigma_r^2 a_i (x_i - w_i) \tag{16d}$$

$$x_i \geq w_i \geq 0,\ y_i \geq 0, \quad i = 1, \cdots, N_1 \tag{16e}$$

where $\mathbf{t} = [t_1, \cdots, t_{N_1}]^T$. Although $\log(1+t_i)$ is a concave function of t_i, constraints in (16b) cannot be proven to be convex. Therefore, the problem (16) is a nonconvex problem. In this paper, we apply the sequential quadratic programming (SQP) [14] method to solve the problem in (16). The complexity order of solving each QP subproblem through the primal-dual potential reduction approach is $\mathcal{O}((4N_1)^{4.5})$. The overall complexity of the SQP approach relies also on the number of iterations required, which depend on the given batch of data. Considering that the complexity of obtaining the SVDs of $\mathbf{H}$ and $\mathbf{G}$ is $\mathcal{O}(N_r^3 + N_s^2 N_r)$ and $\mathcal{O}(N_d^3 + N_r^2 N_d)$, respectively, the total computational complexity order of solving the system design problem (9) through method 1 is $\mathcal{O}(N_r^3 + N_s^2 N_r + N_d^3 + N_r^2 N_d + c_1 (4N_1)^{4.5})$, where c_1 is the number of iterations in the SQP approach.

B. Proposed Method 2

This method converts the problem (15) to a convex problem by exploiting the following upper bound

$$\frac{a_i w_i b_i y_i}{1+a_i w_i + b_i y_i} \leq \frac{a_i w_i b_i y_i}{a_i w_i + b_i y_i}. \tag{17}$$

Using (17), the problem (15) can be converted to

$$\max_{\mathbf{w},\mathbf{x},\mathbf{y},\mathbf{t}} \sum_{i=1}^{N_1} \log(1+t_i) \tag{18a}$$

$$\text{s.t. } \frac{a_i w_i b_i y_i}{a_i w_i + b_i y_i} \geq t_i,\ i = 1, \cdots, N_1 \tag{18b}$$

$$\sum_{i=1}^{N_1} x_i \leq P \tag{18c}$$

$$\sum_{i=1}^{N_1} y_i \leq \eta \sum_{i=1}^{N_1} \sigma_r^2 a_i (x_i - w_i) \tag{18d}$$

$$x_i \geq w_i \geq 0,\ y_i \geq 0, \quad i = 1, \cdots, N_1. \tag{18e}$$

Now we show constraints in (18b) can be converted to semidefinite constraints. From (18b) we have

$$\frac{a_i w_i b_i y_i}{a_i w_i + b_i y_i} - t_i = \frac{(a_i w_i + b_i y_i)^2 - a_i^2 w_i^2 - b_i^2 y_i^2}{2(a_i w_i + b_i y_i)} - t_i \geq 0. \tag{19}$$

Inequality (19) is equivalent to

$$a_i w_i + b_i y_i - a_i w_i (a_i w_i + b_i y_i)^{-1} a_i w_i$$
$$- b_i y_i (a_i w_i + b_i y_i)^{-1} b_i y_i - 2t_i \geq 0$$

which can be rewritten as the following semidefinite constraint

$$\begin{pmatrix} a_i w_i + b_i y_i - 2t_i & a_i w_i & b_i y_i \\ a_i w_i & a_i w_i + b_i y_i & 0 \\ b_i y_i & 0 & a_i w_i + b_i y_i \end{pmatrix} \geq 0. \tag{20}$$

By substituting (18b) with (20), we obtain the following optimization problem

$$\max_{\mathbf{w},\mathbf{x},\mathbf{y},\mathbf{t}} \sum_{i=1}^{N_1} \log(1+t_i) \tag{21a}$$

$$\text{s.t. } \begin{pmatrix} a_i w_i + b_i y_i - 2t_i & a_i w_i & b_i y_i \\ a_i w_i & a_i w_i + b_i y_i & 0 \\ b_i y_i & 0 & a_i w_i + b_i y_i \end{pmatrix} \geq 0$$
$$i = 1, \cdots, N_1 \tag{21b}$$

$$\sum_{i=1}^{N_1} x_i \leq P \tag{21c}$$

$$\sum_{i=1}^{N_1} y_i \leq \eta \sum_{i=1}^{N_1} \sigma_r^2 a_i (x_i - w_i) \tag{21d}$$

$$x_i \geq w_i \geq 0,\ y_i \geq 0, \quad i = 1, \cdots, N_1. \tag{21e}$$

The problem in (21) is a convex nonlinear SDP problem and can be solved by the disciplined convex programming toolbox CVX [15]. The computational complexity of solving this class of problems is an active research area [17]. It can be shown using the results in [17] that by using the augmented Lagrangian method, the problem in (21) can be solved at a complexity order of $\mathcal{O}(c_2 N_1 (6N_1 + 2)^3)$, where c_2 denotes the number of iterations required till convergence. Therefore, considering the complexity of obtaining the SVDs of $\mathbf{H}$ and $\mathbf{G}$, the overall complexity of solving the problem in (9) by method 2 is $\mathcal{O}(N_r^3 + N_s^2 N_r + N_d^3 + N_r^2 N_d + c_2 N_1 (6N_1 + 2)^3)$. Thus, the complexity of the proposed method 2 is lower than that of the proposed method 1.

IV. Simulations

We show the performance of the two proposed transceiver design methods via numerical simulations in this section. We simulate a system where the three nodes are placed in a line as illustrated in Fig. 2. The source-destination distance is set to be $D_{sd} = 20$ meters. The source-relay distance is $D_{sr} = 10k$ meters, while the relay-destination distance is $D_{rd} = 10(2-k)$ meters, where $0 < k < 2$ is normalized over 10 meters. This normalization enables an easy identification of whether the relay is placed nearby the destination node ($1 < k < 2$) or closer to the source node ($0 < k < 1$).

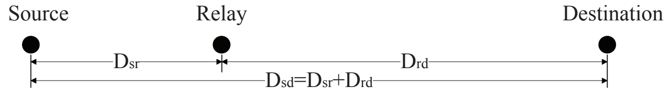

Fig. 2. Locations of the source, relay, and destination nodes.

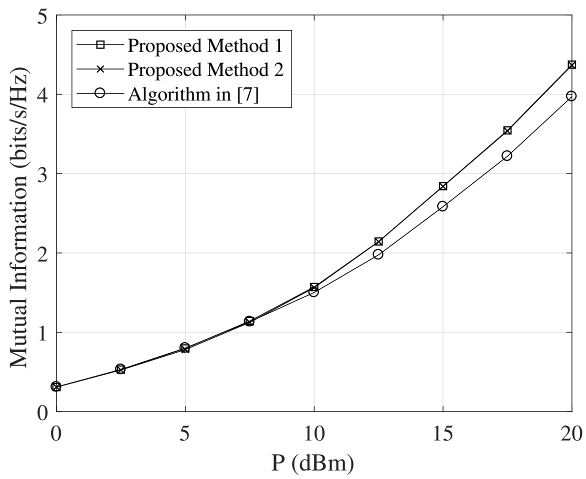

Fig. 3. Example 1: MI versus P, $N = 3$, $k = 1$.

The channel $\mathbf{H}$ and $\mathbf{G}$ have independent and identically distributed complex Gaussian entries as $\mathcal{CN}(0, 1/(N_s L_{sr}))$ and $\mathcal{CN}(0, 1/(N_r L_{rd}))$, respectively, where L_{sr} and L_{rd} are path losses modeled as $L_{sr} = D_{sr}^{\zeta} = (10k)^{\zeta}$ for the source-relay channel and $L_{rd} = D_{rd}^{\zeta} = (10(2-k))^{\zeta}$ for the relay-destination channel. Here $\zeta = 3$ is the path loss exponent. In the numerical simulations, we set $0.25 < k < 1.75$ such that $D_{sr} > 1$ and $D_{rd} > 1$. The noise variances at the relay node and the destination node are set as $\sigma_r^2 = \sigma_d^2 = -50$ dBm. For all numerical examples, we choose $N_s = N_r = N_d = N_1 = N$ and $\eta = 0.8$. We compare the system MI performance of the two proposed methods with the system in [7]. All numerical simulation results are averaged over 1000 independent realizations of channel matrices $\mathbf{H}$ and $\mathbf{G}$.

In our first numerical simulation example, we choose $k = 1$. The MI achieved by the three methods tested versus the source power P is illustrated in Fig. 3 for $N = 3$. We can observe from Fig. 3 that the two proposed methods have a higher system MI than the per date stream power constraints based algorithm in [7]. In particular, the MI gap between the two proposed methods and the algorithm in [7] increases with P. The simulation results indicate that it is important to consider a sum power constraint at the relay node during the system optimization.

Fig. 4 illustrates the MI of the three methods tested versus the source power P for $N = 5$. Similar to Fig. 3, we can see from Fig. 4 that the two proposed methods yield a higher MI than the algorithm in [7]. Moreover, we can see from Figs. 3 and 4 that the achievable MI of the two proposed methods is very close to each other. This can be explained below. For the proposed upper bound based method, the bounding error

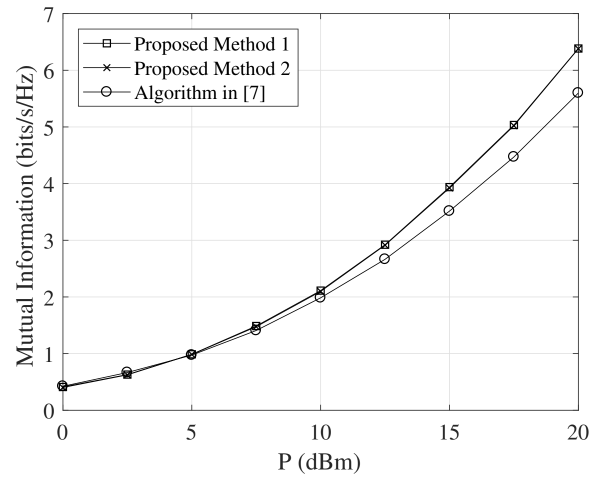

Fig. 4. Example 1: MI versus P, $N = 5$, $k = 1$.

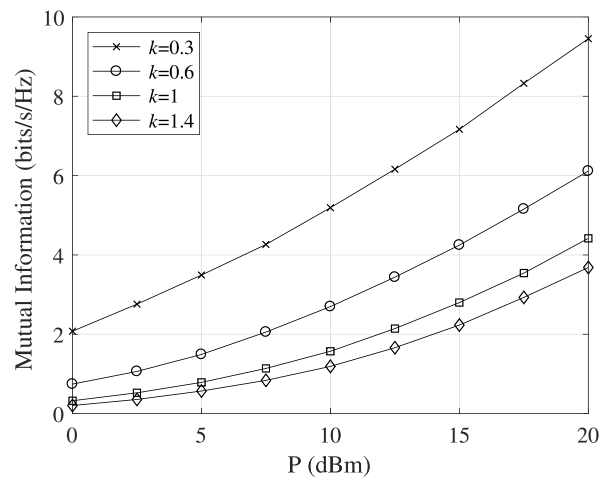

Fig. 5. Example 2: MI of the proposed method 1 versus P at different k, $N = 3$.

in (17) is very small as $a_i w_i$ and $b_i y_i$ are much larger than 1 in real WPC environments. Thus, the two proposed methods converge to the same performance as as P increases. Based on Fig. 3 and Fig. 4, we can observe that the system MI increases when the number of antennas increases, which reflects the benefit of MIMO systems.

In the second numerical example, we investigate the system MI at different source-relay distances. We choose $N = 3$ and investigate the system MI at different k. Fig. 5 illustrates the MI of the proposed method 1 versus P at different k. The MI of the other proposed method is not demonstrated in Fig. 5 as it is similar to the proposed method 1. Fig. 6 illustrates the MI of the three methods tested versus k at $P = 15$dBm and $N = 3$. We can observe from Figs. 5 and 6 that for the three methods tested, the system MI decreases when k increases. This is expected as the relay node can harvest more energy when it gets closer to the source node, and consequently, the MI is higher. We can also see from Fig. 6 that the achievable

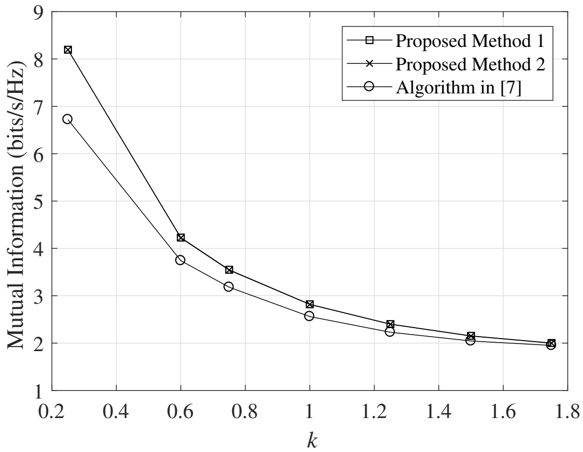

Fig. 6. Example 2: MI versus k, $P = 15$dBm, $N = 3$.

MI of the two proposed methods is higher than the algorithm in [7] for each k, particularly when k is small.

V. Conclusions

We have investigated the joint source matrix, relay matrix, and PS ratio design for a MIMO AF relay system with a PS-based EH relay node. Compared with the per data stream energy constraints at the relay node adopted by existing approaches, we have proposed a general sum energy constraint at the relay node. The structure of the optimal source matrix and relay matrix has been obtained which reduces the difficult joint transceiver design problem to a simpler joint source and relay power allocation problem. Two methods have been developed to solve the power allocation problem, where one method yields a higher system MI than the other method at the cost of a higher complexity. Numerical simulations show that the two proposed methods have higher system MI than the per data stream power constraint based method.

Appendix

We first show that the optimal structure of $\mathbf{B}$ in (11) maximizes the right-hand side of (9c). This can be formulated as the problem below

$$\max_{\mathbf{B}} \ \mathrm{tr}((\mathbf{I}_{N_1} - \mathbf{D})\mathbf{\Lambda}_{h,1}^{\frac{1}{2}}\mathbf{V}_{h,1}^H\mathbf{B}\mathbf{B}^H\mathbf{V}_{h,1}\mathbf{\Lambda}_{h,1}^{\frac{1}{2}}) \quad (22a)$$

$$\text{s.t.} \ \mathrm{tr}(\mathbf{B}\mathbf{B}^H) \leq P. \quad (22b)$$

By introducing $\tilde{\mathbf{D}} = (\mathbf{I}_{N_1} - \mathbf{D})\mathbf{\Lambda}_{h,1}$, the problem (22) can be written as

$$\max_{\mathbf{B}} \ \mathrm{tr}(\mathbf{V}_{h,1}\tilde{\mathbf{D}}\mathbf{V}_{h,1}^H\mathbf{B}\mathbf{B}^H) \quad (23a)$$

$$\text{s.t.} \ \mathrm{tr}(\mathbf{B}\mathbf{B}^H) \leq P. \quad (23b)$$

From Proposition 2.1 of [2], the solution to the problem (23) satisfies $\mathbf{B}^*\mathbf{B}^{*H} = P\mathbf{v}_{h,1}\mathbf{v}_{h,1}^H$, where $\mathbf{v}_{h,1}$ is the first column of $\mathbf{V}_h$ [2]. This means $\mathbf{B}^*$ is a rank-one matrix as $\mathbf{B}^* = P^{\frac{1}{2}}\mathbf{v}_{h,1}\mathbf{u}_1^H$, where $\mathbf{u}_1$ is an $N_1 \times 1$ vector with $\mathbf{u}_1^H\mathbf{u}_1 = 1$. Apparently, this is a special case of $\mathbf{B}^* = \mathbf{V}_{h,1}\mathbf{\Lambda}_b^{\frac{1}{2}}\mathbf{U}^H$ in (11) when $\mathbf{\Lambda}_b = \mathrm{diag}(P, 0, \cdots, 0)$ and the first column of $\mathbf{U}$ is $\mathbf{u}_1$. In other words, (11) is optimal for the problem (23).

Secondly, for any value of $\eta\mathrm{tr}((\mathbf{I}_{N_1} - \mathbf{D})\tilde{\mathbf{B}}\tilde{\mathbf{B}}^H) = P_r$, the problem (9) can be written as

$$\max_{\mathbf{D},\mathbf{B},\mathbf{F}} \ \mathrm{MI}(\mathbf{D}, \mathbf{B}, \mathbf{F}) \quad (24a)$$

$$\text{s.t.} \ \mathrm{tr}(\mathbf{B}\mathbf{B}^H) \leq P \quad (24b)$$

$$\mathrm{tr}(\mathbf{F}(\mathbf{D}^{\frac{1}{2}}\tilde{\mathbf{B}}\tilde{\mathbf{B}}^H\mathbf{D}^{\frac{1}{2}} + \sigma_r^2\mathbf{I}_{N_r})\mathbf{F}^H) \leq P_r. \quad (24c)$$

It can be seen that for *any* $P_r > 0$, the problem (24) is in the same form as the joint source matrix and relay matrix optimization problem (13)-(15) in [19] with a first-hop channel of $\mathbf{D}^{\frac{1}{2}}\mathbf{\Lambda}_{h,1}^{\frac{1}{2}}\mathbf{V}_{h,1}^H$ and a second-hop channel of $\mathbf{G}$. Thus, based on Theorem 1 in [19], the structure of $\mathbf{B}^*$ and $\mathbf{F}^*$ in (11) are proven. □

References

[1] L. R. Varshney, "Transporting information and energy simultaneously," in *Proc. IEEE Int. Symp. Inf. Theory (ISIT)*, Toronto, Canada, July 6-11, 2008, pp. 1612-1616.

[2] R. Zhang and C. K. Ho, "MIMO broadcasting for simultaneous wireless information and power transfer," *IEEE Trans. Wireless Commun.*, vol. 12, pp. 1989-2001, May 2013.

[3] B. Li, Y. Rong, J. Sun, and K. L. Teo, "A distributionally robust linear receiver design for multi-access space-time block coded MIMO systems," *IEEE Trans. Wireless Commun.*, vol. 16, pp. 464-474, Jan. 2017.

[4] Y. Rong, "Joint source and relay optimization for two-way linear non-regenerative MIMO relay communications," *IEEE Trans. Signal Process.*, vol. 60, pp. 6533-6546, Dec. 2012.

[5] B. K. Chalise, W. K. Ma, Y. D. Zhang, H. Suraweera, and M. G. Amin, "Optimum performance boundaries of OSTBC based AF-MIMO relay system with energy harvesting receiver," *IEEE Trans. Signal Process.*, vol. 61, pp. 4199-4213, Sep. 2013.

[6] Z. Ding, C. Zhong, D. W. K. Ng, M. Peng, H. A. Suraweera, R. Schober, and H. V. Poor, "Applications of smart antenna technologies in simultaneous wireless information and power transfer," *IEEE Commun. Mag.*, vol. 53, pp. 86-93, Apr. 2015.

[7] K. Xiong, P. Fan, C. Zhang, and K. B. Letaief, "Wireless information and energy transfer for two-hop non-regenerative MIMO-OFDM relay networks," *IEEE J. Select. Areas Commun.*, vol. 26, pp. 1397-1407, Aug. 2015.

[8] Z. Chu, M. Johnston, and S. Le Goff, "SWIPT for wireless cooperative networks," *Electronics Lett.*, vol. 51, no. 6, pp. 536-538, Mar. 19, 2015.

[9] Z. Wen, X. Liu, N. C. Beaulieu, R. Wang, and S. Wang, "Joint source and relay beamforming design for full-duplex MIMO AF relay SWIPT systems," *IEEE Commun. Lett.*, vol. 20, pp. 320-323, Feb. 2016.

[10] G. Amarasuriya, E. G. Larsson, and H. V. Poor, "Wireless information and power transfer in multiway massive MIMO relay networks," *IEEE Trans. Wireless Commun.*, vol. 15, pp. 3837-3855, June 2016.

[11] B. Li and Y. Rong, "Joint transceiver optimization for wireless information and energy transfer in non-regenerative MIMO relay systems," *IEEE Trans. Veh. Technol.*, vol. 67, pp. 8348-8362, Sep. 2018.

[12] B. Li, H. Cao, Y. Rong, T. Su, G. Yang, and Z. He, "Transceiver optimization for DF MIMO relay systems with a wireless powered relay node," *IEEE Access*, vol. 7, pp. 56904-56919, Apr. 2019.

[13] J. L. Bing, Y. Rong, L. Gopal, and C. W. R. Chiong, "Transceiver design for SWIPT MIMO relay systems with hybridized power-time splitting-based relaying protocol," *IEEE Access*, vol. 8, pp. 190922-190933, Oct. 2020.

[14] D. P. Bertsekas, *Nonlinear Programming*. Belmont, MA: Athena Scientific, 1995.

[15] M. Grant and S. Boyd, "The CVX Users Guide," Release 2.1, Oct. 2014. [Online]. Available: http://web.cvxr.com/cvx/doc/CVX.pdf.

[16] X. Tang and Y. Hua, "Optimal design of non-regenerative MIMO wireless relays," *IEEE Trans. Wireless Commun.*, vol. 6, no. 4, pp. 1398-1407, Apr. 2007.

[17] M. Stingl, "On the solution of nonlinear semidefinite programs by augmented Lagrangian methods," Ph.D. dissertation, University of Erlangen-Nuremberg, Germany, 2006.

[18] X. Lu, D. Niyato, P. Wang, D. I. Kim, and Z. Han, "Wireless charger networking for mobile devices: Fundamentals, standards, and applications," *IEEE Wireless Commun.*, vol. 22, pp. 126-135, Apr. 2015.

[19] Y. Rong, X. Tang, and Y. Hua, "A unified framework for optimizing linear non-regenerative multicarrier MIMO relay communication systmes," *IEEE Trans. Signal Process.*, vol. 6, no. 12, pp. 4837-4851, Dec. 2009.